Physical modelling studies of the effect of surcharge on the behavior of geogrid reinforced soil walls

R. Linhares, M. Ehrlich, S. H. Mirmoradi & L. P. de Oliveira
Dept. of Civil Engineering, COPPE, Federal University of Rio de Janeiro, Brazil

ABSTRACT: A physical model study of the effect of surcharge width on the behavior of geosynthetic-reinforced soil GRS walls was carried out. Surcharges up to 100 kPa with three different widths were applied to the top of GRS walls, strip loadings of 0.6 m and 1.2 m width, and also to the entire surface, starting from the back of the face. The walls were well instrumented to measure the reinforcement load, the block facing lateral movement and the settlements. The results show that the maximum reinforcement load, lateral displacement of the facing and settlements were affected significantly by the width of the surcharge. Moreover, a decrease in the surcharges width led to both the locations of the maximum load in reinforcements and settlements near the facing.

Keywords: GRS walls, physical modelling, surcharge width, reinforcement tension, facing lateral displacement, settlement

1 INTRODUCTION

Many studies, both physical and theoretical (numerical and analytical), have been conducted in past decades to better understand the effect of some factors on the behavior of geosynthetic reinforced soil (GRS) walls. The wall construction characteristics, such as the facing type and inclination, reinforcement type, stiffness and spacing, resistance and compaction of the backfill soil may greatly influence the load and strain in reinforcements and the lateral displacements of the wall facing and settlements (Tatsuoka, 1993; Ehrlich & Mitchell, 1994; Helwany et al., 1999, Huang et al., 2010; Stuedlein et al., 2012; Ehrlich & Mirmoradi, 2013; Mirmoradi & Ehrlich, 2015; Riccio et al., 2014; Allen & Bathurst, 2015; Vahedifard et al., 2016; Mirmoradi et al.; 2016). However, the surcharge characteristics, such as its magnitude, position and geometry, may significantly affect the GRS wall behavior (Gomes et al, 1994; Palmeira et al, 1996; Abu-Hejleh et al, 2000; Ambauen et al., 2015; Mirmoradi, 2015; Xiao et al, 2016).

The surcharge location changes the failure mechanisms (Gomes et al, 1994). Additionally, past studies have shown that the closer the surcharge is to the face: (i) the greater the value of the lateral earth pressure in the back of the facing (Ambauen et al., 2015); and (ii) the greater the value of maximum reinforcement load (T_{max}), settlement, toe load and lateral displacements (Mirmoradi, 2015). The surcharge position, reinforcement stiffness (Ambauen et al. 2015) and toe lateral restrain (Mirmoradi, 2015) affect the T_{max} value and tension distribution along reinforcements.

In this study, three large-scale GRS walls were constructed at COPPE/UFRJ facilities. The walls were the same except for the surcharge width. The effect of surcharge width in the reinforcement load, lateral displacements and settlements is shown.

2 TESTS CHARACTERISTICS AND MATERIAL USED

Three physical models of reinforced soil walls 1.2 m high were built at the Geotechnical Laboratory of COPPE/UFRJ. The constructions of all GRS walls followed the same procedures, the only difference between them was the surcharge width applied at the top of the walls: Wall 1 (q_1), 0.6 m width from the

back of the face; Wall 2 (q_2), 1.2 m width from the back of the face; Wall 3 (q_t), entire surface. Fig. 1 presents the physical models' cross-section and the different applied surcharges.

In all walls, three layers of a flexible polyester geogrid were installed along their height, placed at 0.2 m, 0.6 m, and 1.0 m above the wall bottom. The geogrid length and vertical spacing were 2.3 m and 0.4 m, respectively. The reinforcements' mechanical properties were provided by the company and are shown in Table 1.

The wall facing was composed of precast blocks with an inclination equal to 6° to the vertical. Fig. 2 illustrates the backfill material's particle-size distribution curve, a well-graded sand made artificially from crushed quartz powder with D_{50} of 0.25 mm, curvature coefficient C_c of 1.0, uniformity coefficient C_u of 8.9 and a plasticity index (PI) of zero.

The soil was compacted using a light vibrating plate with equivalent static load of 8 kPa, ensuring a unit weight after compaction of 21 kN/m^3 (Saramago, 2002, Ehrlich et al. 2012). The soil friction angles were determined by triaxial and plane-strain tests as 42° and 50°, respectively (Costa, 2005, Ehrlich et al. 2012).

A 1.0 m wide lubricated zone composed of rubber sheets and Teflon grease was placed at the bottom of the wall, including the base of the block facing, allowing potential failure surface movement and keeping it away from the face of the wall. The same lubrication system was applied to the internal facing of the U-shaped concrete box in which the walls were built, reducing the lateral friction and approaching a plane-strain condition for the physical model (Saramago, 2002, Ehrlich et al. 2012).

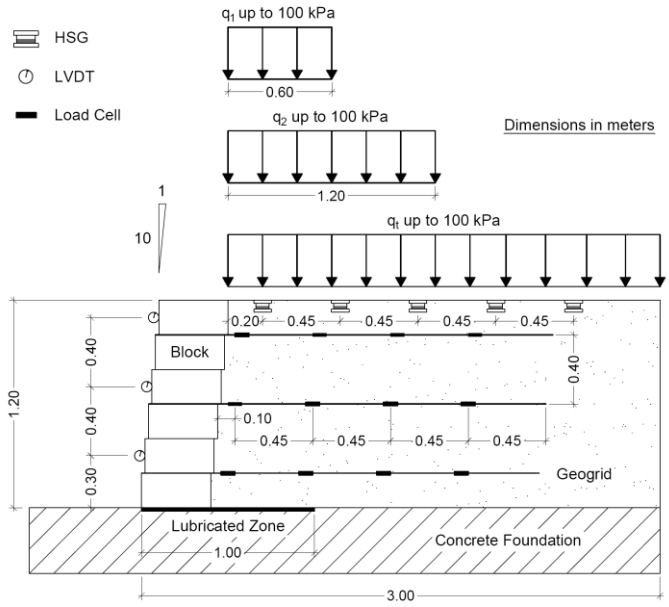

Figure 1. Cross-section of physical models and surcharges applied.

Table 1. Mechanical and physical properties of reinforcement.

Longitudinal tensile strength (kN/m)	≥55
Transverse tensile strength (kN/m)	≥25
Elongation (%)	≤6
Weight (g/m²)	240
Opening size (mm)	20x30

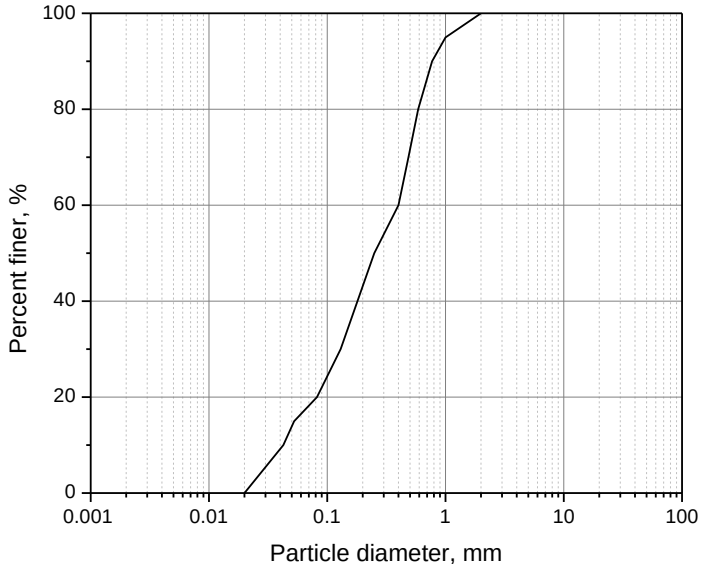

Figure 2. Particle-size distribution curve.

3 CONSTRUCTION SEQUENCE AND SURCHARGE APPLICATION

The construction was executed in six layers of soil, each one 0.2 m thick, and by building a 1.2 m high wall. Firstly, the soil was simply placed and then compacted for 10 minutes with a light vibrating plate. The reinforcements were installed at the top of the 1st, 3rd and 5th layers (see Fig. 1). Every reinforcement layer was divided into three sections, with the central part, 0.5 m wide, the only one instrumented. Using air bags and a reaction system, the surcharges were applied from the back of the facing to: a 0.6 m wide zone (q_1); a 1.2 m wide zone (q_2); and the entire surface of the backfill soil (q_t), all starting from the back of the face (see Fig. 1). Each surcharge application occurred in a new, untested wall.

4 INSTRUMENTATION

Fig. 1 also presents the instrumentation used in all tests. There were four pairs of load cells in each layer of reinforcement (totalizing 24 load cells) to monitor the reinforcement load, three linear variable differential transformers (LVDTs) to monitor the lateral facing displacement and five hydraulic settlement gauges (HSGs) to monitor the vertical displacement at the top surface of the wall.

5 TESTS RESULTS

5.1 *Reinforcement loads*

Fig. 3(a) shows for Walls 1, 2 and 3 the sum of maximum reinforcement loads, ΣT_{max}, during the surcharge application. For better comparison of the behavior of the walls during loading, the curves were modified considering the same value of ΣT_{max} at the end of construction (EOC) (Fig. 3b). The results show that the higher the width and value of the surcharge, the steeper the curves. The value of the ΣT_{max} at 100 kPa (End of Loading, EOL), observed in Wall 3 (q_t), was 20% and 9% greater than Wall 1 (q_1) and Wall 2 (q_2), respectively. This result agrees with Ambauen et al. (2015) and Mirmoradi (2015).

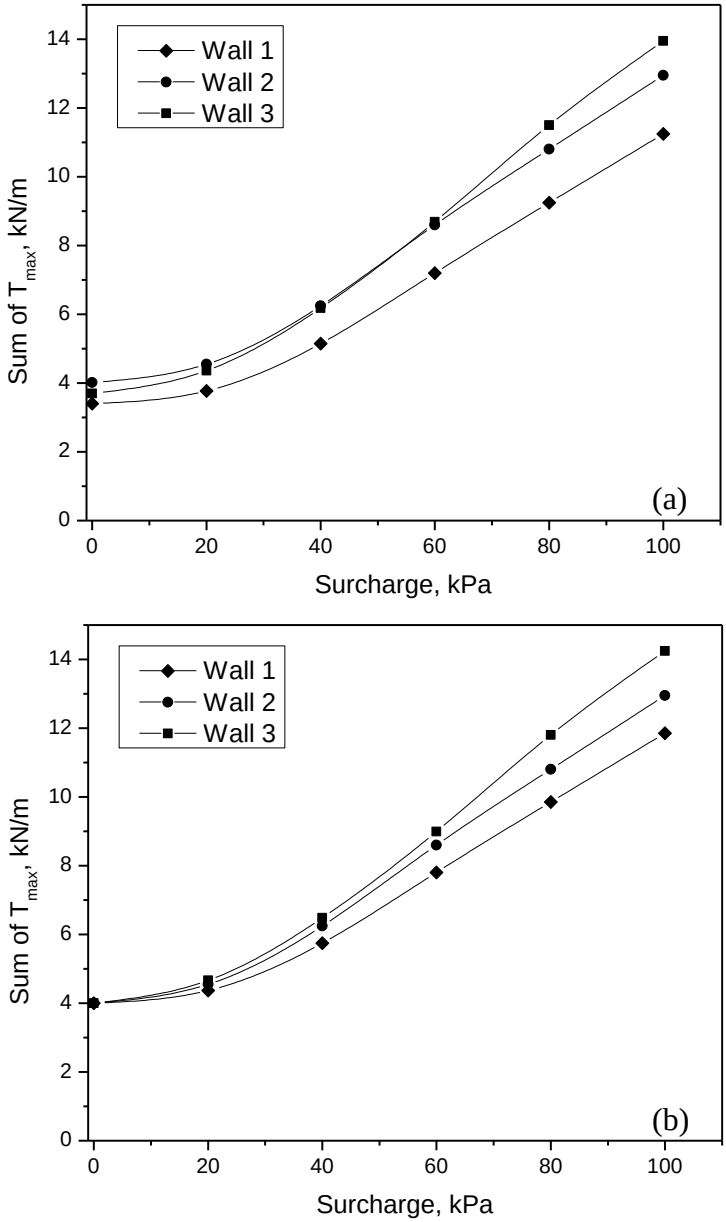

Figure 3. (a) ΣT_{max} and (b) modified ΣT_{max} values versus surcharge.

Fig. 4 shows the reinforcement loads at three different loading stages (EOC, 60 kPa and EOL). In all loading conditions, T_{max} was located further from the facing in the reinforcement layer placed at the bottom of the wall and close to the back of facing in the upper layers. The wider the loading, the higher the T_{max} value in the reinforcement placed at the bottom of the walls. On the other hand, in the other layers the T_{max} values were more similar. The notable difference in the distribution of load along the reinforcement was observed in Wall 1 (q_1) at the third location of load measurement from the back of the facing, indicating that for this condition the reinforcement load is more concentrated near the face and does not mobilize tensions in reinforcements beyond its limits, as observed by Abu-Hejleh et al. (2000).

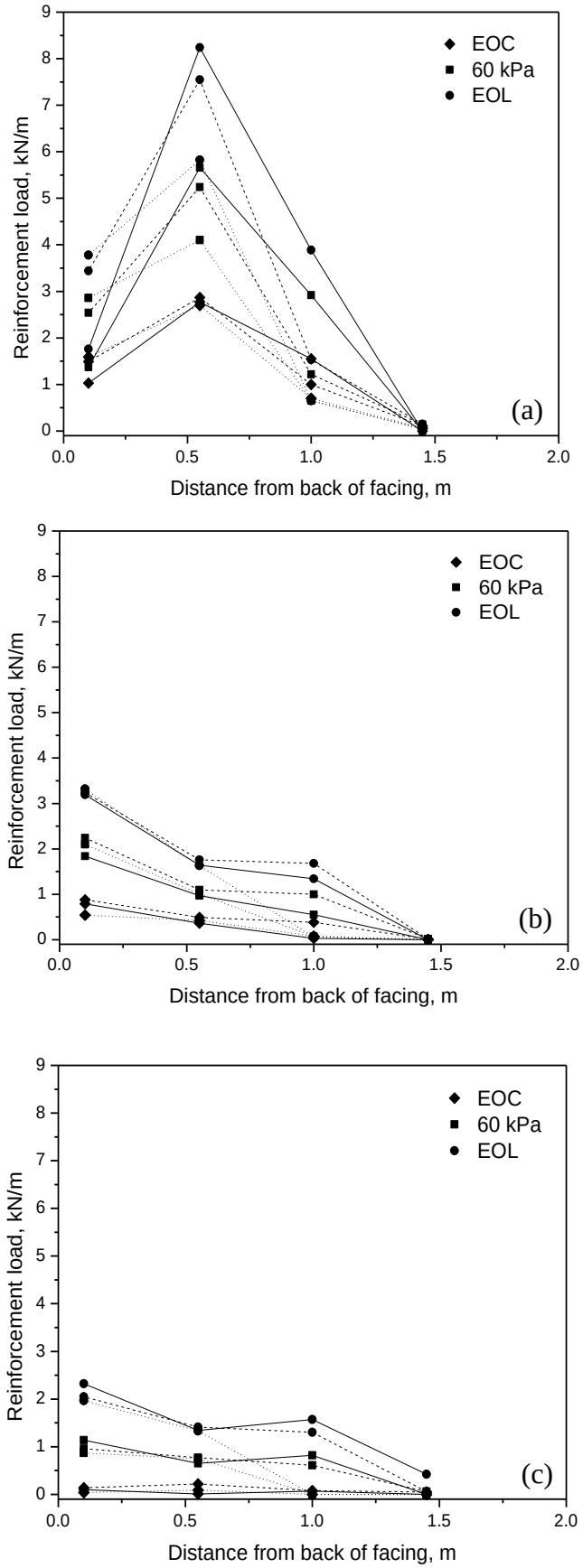

Figure 4. Loads in the reinforcement layers: (a) placed at the bottom; (b) middle; and (c) top of the walls at EOC, 60 kPa and EOL. Wall 1 (dotted lines); Wall 2 (dashed lines); and Wall 3 (solid lines).

5.2 *Horizontal facing displacement*

Fig. 5 shows the average horizontal displacement increment (ΔH_{ave}) during the surcharge application for Walls 1 and 3. Owing to an instrument malfunction, there is no data from Wall 2. Wall 3 presented higher values of ΔH_{ave}. Furthermore, the difference of ΔH_{ave} measured in the two walls increased with the increase in loading, as observed by Mirmoradi (2015).

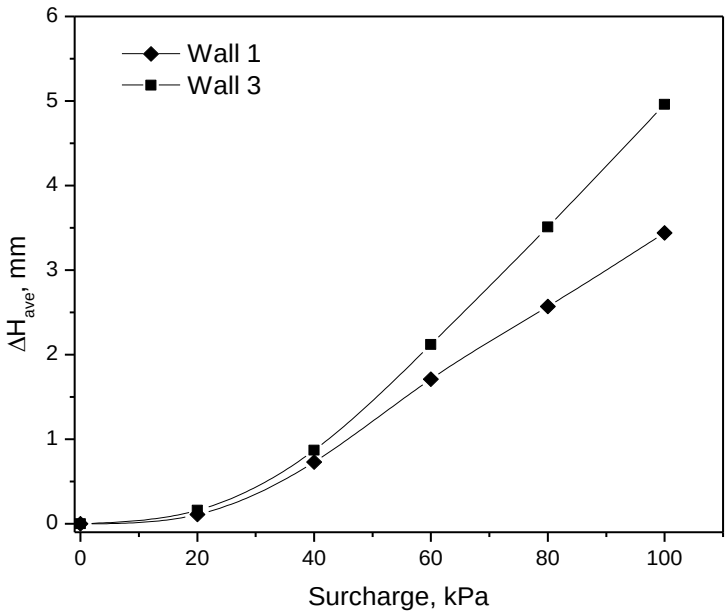

Figure 5. Average horizontal displacements increment (ΔH_{ave}) during surcharge application.

5.3 *Settlements*

Fig. 6 presents the settlements at the top of Walls 1, 2 and 3 at the EOL. For all walls, the highest settlement was observed close to the wall facing. Wall 1 (q_1) presented the highest value of settlement near to the block face, and with the distance from the facing an abrupt decreased was observed, being close to zero at 1.10 m distance. In Wall 2, the settlements were close to zero at 1.55 m from the wall facing. In Wall 3, a lower decrease in the settlements occurred with the distance from the facing.

The curves were integrated in order to analyze the total vertical displacement of all walls. Wall 3 presented the highest value (3746 mm²), followed by Wall 2 (2488 mm²), and lastly, Wall 1 (2129 mm²), indicating that the wider the load, the higher the impact of the settlements. These results agree with Ambauen et al. (2015).

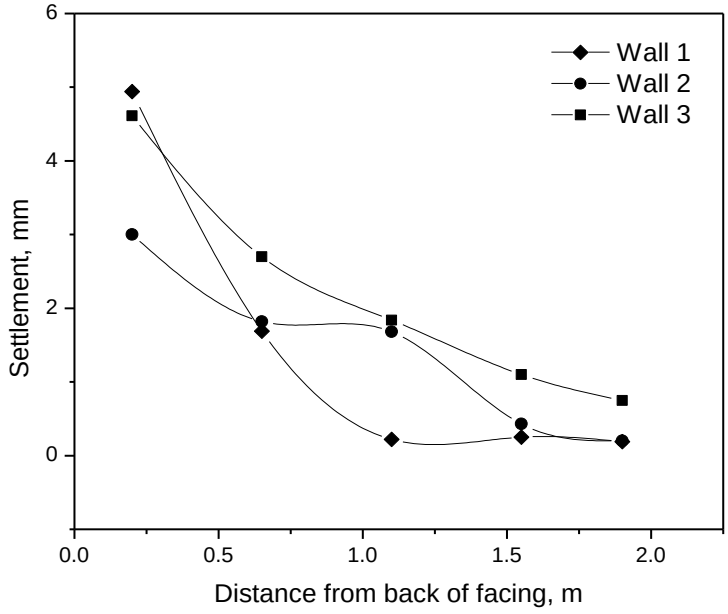

Figure 6. Settlements at final stage of loading (100 kPa).

6 SUMMARY AND CONCLUSIONS

Three large-scale physical models were built at the Geotechnical Laboratory of COPPE/UFRJ to experimentally evaluate the effect of surcharge width on GRS wall behavior. The construction of all GRS walls followed the same procedure: the only difference between them was the width of the surcharge, starting from the back of the face. Instruments were installed to monitor the reinforcement loads, settlements and the lateral displacement of the facing.

The results indicate that the decrease in the width of the surcharge led to a more concentrated load in reinforcement and settlements near to the face. The lateral displacements at the top of the wall also tended to be higher. Note that the mobilized tension at the top reinforcement layer was more affected by the width of the surcharge. Moreover, the wider the surcharge, the higher the values of T_{max}, average lateral displacements and settlements.

REFERENCES

Abu-Hejleh, N., Wang, T., & Zornberg, J. 2000. Performance of Geosynthetic-Reinforced Walls Supporting Bridge and Approaching Roadway Structures. ASCE/Geotechnical Special Publication No. 103, Advances in Transportation and Geoenvironmental Systems Using Geosynthetics, Proceeding of Sessions of GEO-Denver 2000, Denver, USA, p. 218-243.

Allen, T.M., & Bathurst, R.J. 2015. An improved simplified method for prediction of loads in reinforced soil walls. ASCE J. Geotechinical and Geoenvironmental Engineering: ASCE, Vol. 141(11): 04015049.

Ambauem, S, Leshchinsky, B. Xie, Y, & Rayamajhi, D. 2015. Service-state behavior of reinforced soil walls supporting spread footings: a parametric study usinf finite-element analysis. Geosynthetics International. http://dx.doi.org/10.1680/jgein.15.00039.

Costa, R.S. Um novo equipamento triaxial para ensaios de solos na condição de deformação plana. COPPE/UFRJ. Master dissertation, Rio de Janeiro, Brazil, 157 p.

Ehrlich, M., Mirmoradi, S. H., and Saramago, R. P., 2012. Evaluation of the effect of compaction on the behavior of geosynthetic-reinforced soil walls. J. Geotextile Geomembr. 34(Oct): 108-115.

Ehrlich, M., & Mirmoradi, S.H. 2013. Evaluation of the Effects of Facing Stiffness and Toe Resistance on the Beahvior of GRS Walls. Journal Geotextiles and Geomembranes: IGS, Vol. 40, p. 28-36.

Ehrlich, M., & Mitchell, J.K. 1994. Working stress design method for reinforced soil walls. Journal of Geotechnical Engineering: ASCE, Vol. 120, N. 4, p. 625-6454.

Gomes, R.C., Palmeira, E.M., & Lanz, D. 1994. Failure and Deformation Mechanisms in Model Reinforced Walls Subjected to Different Loading Conditions. Geosynthetics International, Vol. 1 (1), p. 45-65.

Helwany, S.M.B., Reardon, G., & WU, J.T.H. 1999. Effects of backfill on the performance of GRS retaining walls. Geotextiles and Geomembranes: IGS, Vol. 17, p. 1-16.

Huang, B., Bathurst, R.J., Hatami, K., & ALLEN, T.M. 2010. Influence of toe restraint on reinforced soil segmental walls. Canadian Geotechnical Journal, Vol. 47, p 885-904.

Mirmoradi, S.H., Ehrlich, M. 2015. Numerical evaluation of the behavior of GRS walls with segmental block facing under working stress conditions. Geotechnical and Geoenvironmental Engineering: ASCE, Vol. 141, p. 04014109.

Mirmoradi, S.H., Ehrlich, M., & Dieguez, C. 2016. Evaluation of the combined effect of toe resistance and facing inclination on the behavior of GRS wall. Geotextiles and Geomembranes: IGS, Vol. 44, p. 287-294.

Mirmoradi, S.H. 2015 Evaluation of the Behavior of Reinforced Soil Walls Under Working Stress Condition. COPPE/UFRJ. Phd thesis, Rio deJaneiro, Brazil, 340 p.

Palmeira, E.M., & Gomes, R.C., 1996. Comparisons of predicted and observed failure mechanisms in model reinforced soil walls. Geosynthetics International, Vol. 3 (3), p. 329-347.

Riccio, M., Ehrlich, M., & Dias, D. 2014. Field monitoring and analyses of the response of a block-faced geogrid wall using fine-grained tropical soils. Journal of Geotextiles and Geomembranes: IGS., Vol. 42 (2), p. 127-138.

Saramago, R.P. 2002. Estudo da influência da compactação no comportamento de muros de solo reforçado com a utilização de modelos físicos. COPPE/UFRJ. Phd thesis, Rio deJaneiro, Brazil, 294 p.

Stuedlein, A.W., Allen, T.M., Holtz, R.D., & Christopher, B.R. 2012. Assessment of reinforcement strains in very tall mechanically stabilized earth walls. Journal of Geotechnical and Geoenvironmental Engineering: ASCE, Vol. 138 (3), p. 345-356. Doi:10.1061/(ASCE)GT.1943-5606.0000586.

Tatsuoka, F. 1993. Keynote lecture: roles of facing rigidity in soil reinforcing. In: Ochiai, Y., Hayashi, S., Otani, J. (Eds.), Earth Reinforcement Practice. Balkema, Rotterdam, p. 831-870.

Vahedifard, F., Shahrokhabadi, S., & Leshchinsky, D. 2016. Geosynthetic-reinforced soil structures with concave facing profile. Geotextiles and Geomembranes: IGS, Vol. 44, p. 358-365.

Xiao, C., Han, J., & Zhang, Z. 2016. Experimental study on performance of geosynthetic-reinforced soil model walls on rigid foundations subjected to static footing loading. Geotextiles and Geomembranes: IGS, Vol. 44 (1), p. 81-94.